Direct measurement of a radially polarized focused evanescent field facilitated by a single LCD

Baohua Jia, Xiaosong Gan, and Min Gu

Centre for Micro-Photonics, Faculty of Engineering and Industrial Sciences, Swinburne University of Technology, P.O. Box 218 Hawthorn, VIC 3122 Australia
xgan@swin.edu.au

Abstract: In this paper, a tightly focused evanescent field produced by a total internal reflection objective lens under the illumination of a radially polarized beam generated using a single liquid crystal phase modulator is investigated. The field distributions have been directly mapped by a scanning near-field optical microscope. It is demonstrated both theoretically and experimentally that the introduction of radially polarized beam illumination combining with an annular beam illumination exhibits advantages in two aspects. On one hand, it corrects the focus elongation and splitting in a focused evanescent field associated with a linearly polarized beam. On the other hand, it significantly improves the lateral localization to approximately a quarter of the illumination wavelength, which is less than half of the size that is achievable under linearly polarized illumination.

References and links

1. J. J. Macklin, J. K. Trautman, T. D. Harris, L. E. Brus, "Imaging and time-resolved spectroscopy of single molecules at an interface," Science **272**, 255-258 (1996).
2. M. Tokunaga, K. Kitamura, K. Saito, A. H. Iwane and T. Yanagida, Biochem. "Single molecule imaging of fluorophores and enzymatic reactions achieved by objective-type total internal reflection fluorescence microscopy," Biophys. Res. Commun. **235**, 47-53 (1997).
3. B. Sick, B. Hecht, and L. Novotny, "Orientational imaging of single molecules by annular illumination, " Phys. Rev. Lett. **85**, 4482-4485 (2000).
4. N. Hayazawa, A. Tarun, Y. Inouye, and S. Kawata, "Near-field enhanced Raman spectroscopy using side illumination optics," J. Appl. Phys. **92**, 6983-6986 (2002).
5. N. Hayazawa, Y. Inouye, and S. Kawata, "Evanescent field excitation and measurement of dye fluorescence in a metallic probe near-field scanning optical microscope," J. Microsc. **194**, 472-476 (1999).
6. J. W. M. Chon and M. Gu, "Scanning total internal reflection fluorescence microscopy under one-photon and two-photon excitation: image formation," Appl. Opt. **43**, 1063-1071 (2004).
7. M. Gu, J.-B. Haumonte, Y. M., J. W. M. Chon, and X. Gan, "Laser trapping and manipulation under focused evanescent wave illumination," Appl. Phys. Lett. **84**, 4236-4238 (2004).
8. D. Ganic, X. Gan, Min Gu, "Trapping force and optical lifting under focused evanescent wave illumination," Opt. Express **12**, 5533-5538 (2004), http://www.opticsexpress.org/abstract.cfm?URI=OPEX-12-22-5533.
9. E. J. Sanchez, L. Novotny, X.S. Xie, "Near-field fluorescence microscopy based on two-photon excitation with metal tips," Phys. Rev. Lett. **82**, 4014-4017 (1999).
10. S. Takahashi, T. Fujimoto, K. Kato, and I. Kojimay, "High resolution photon scanning tunneling microscope," Nanotechnology **8,** A54–A57 (1997).
11. A. Bouhelier, M. R. Beversluis, and L. Novotny, "Near-field scattering of longitudinal fields," Appl. Phys. Lett. **82**, 4596-4598 (2003).
12. B. Jia, X. Gan, and M. Gu, "Direct observation of a pure focused evanescent field of a high numerical aperture objective lens by scanning near-field optical microscopy," Appl. Phys. Lett. **86**, 131110, (2005).
13. Q. Zhan and J. R. Leger, "Focus shaping using cylindrical vector beams," Opt. Express **10**, 324-331 (2002), http://www.opticsexpress.org/abstract.cfm?URI=OPEX-10-7-324.

14. R. Dorn, S. Quabis, and G. Leuchs, "Sharper focus for a radially polarized light beam," Phys. Rev. Lett. **91**, 233901 (2003).
15. A. V. Nesterov, V. G. Niziev, and V. P. Yakunin, "Generation of high-power radially polarized beam," J. Phys. D Appl. Phys. **32**, 2871-2875 (1999).
16. A. A. Tovar, "Production and propagation of cylindrically polarized LaguerreGaussian laser beams," J. Opt. Soc. Am. A, **15**, 27052711 (1998).
17. Z. Bomzon, G. Biener, V. Kleiner, and E. Hasman, "Radially and azimuthally polarized beams generated by space-variant dielectric subwavelength gratings," Opt. Lett. **27**, 285-287 (2002).
18. S. C. Tidwell, D. H. Ford, and W. D. Kimura, "Generating radially polarized beams interferometrically," Appl. Opt. **29**, 2234-2239 (1990).
19. K.S. Youngworth and T.G. Brown, "Focusing of high numerical aperture cylindrical-vector beams," Opt. Express **7**, 77-87 (2000), http://www.opticsexpress.org/abstract.cfm?URI=OPEX-7-2-77.
20. D. P. Biss and T. G. Brown, "Cylindrical vector beam focusing through a dielectric interface," Opt. Express **9**, 490-497 (2001), http://www.opticsexpress.org/abstract.cfm?URI=OPEX-12-5-967.
21. D. Loerke, B. Preitz, W. Stühmer, M. Oheim, "Superresolution measurements by evanescent-wave excitation of fluorescence using variable beam incidence," J. Biomed. Opt. **5**, 23-30 (2000).

1. Introduction

Near-field imaging, sensing and manipulation techniques have become increasingly important in the fields of modern physics, chemistry and biology, especially for studying single molecule dynamics [1-9]. A highly localized evanescent field can be generated by either using a nano-aperture or a metallic tip [4,5,10,11]. However, these methods have the common difficulties, such as a fragile near-field probe, a low throughput and signal-to-noise ratio, and a slow response of gap controlling between the probe and a sample. Recently, near-field optical trapping and imaging techniques using a focused evanescent field generated by an annular beam illuminated total internal reflection (TIR) objective have been proposed and demonstrated [6-8], in which case the fast decaying nature of an evanescent field can localize the field axially to the interface within a 60 nm range. However, a focus elongation or splitting [6,12] in the lateral direction was experienced in this case because a linearly polarized beam was adopted as the illumination. It is well known that when focused by a high numerical aperture (NA) objective, the depolarization effect accompanying with a linearly polarized beam originating from the presence of the longitudinal component in the focal region always results in the deterioration of the lateral resolution and is undesired for most applications. Such a deformation of the focal spot becomes more severe in the near-field region [6,12]. It has been demonstrated in some far-field applications that focus elongation can be removed by introducing a radially polarized illumination [13,14], although at the cost of a poorer axial resolution (a larger depth of focus) due to the dominant portion of the longitudinal electric field component in the focal region of a radially polarized beam [9]. In order to eliminate the focus deformation in the lateral dimension and at the same time axially confine the focal spot in the close vicinity to the interface, a tightly focused evanescent field combining with a radially polarized beam illumination is proposed in this paper.

Radially polarized beams can be generated by various methods, including inserting specially designed elements, a mode converter or a conical element, into a laser resonator [15], or incorporating polarization selective mirrors or a Brewster type window into a high powered laser [16], or using computer-generated space-variant dielectric or metal strip sub-wavelength gratings [17]. In this paper, a radially polarized beam is produced by an interferometric method facilitated by a single liquid crystal phase modulator in order to achieve better synchronization in the dynamic control of the focal spot.

2. Experiment

The radially polarized beam can be generated by the interference of two opposite hand circularly polarized Laguerre-Gaussian (LG) beams of opposite topological charges [18]. The experiment setup is shown in Fig. 1. A single LCD has been adopted instead of two to

generate the LG beams. Two helical phase patterns with opposite spiral directions are loaded simultaneously to a computer controlled spatial light modulator (SLM) (Hamamatsu PPM X8267 Series) to produce LG beams of opposite topological charges (Fig. 1(a) (b)). This method possesses the advantages of better synchronization in the dynamic control of the focal spot and high efficiency. The efficiency of generating the LG beams is approximately 100%, however it is limited by the beamsplitter used in front of the LCD. The generated beams are then split into two arms by another beamsplitter. A polarizer and a quarter wave plate are placed in each arm of the interferometer to convert the linearly polarized LG beams to left-hand and right-hand circularly polarized beams, respectively. The combined radially polarized beam (Fig. 1(c)) is focused by a TIR objective (Olympus, NA=1.65, 100×) at a coverglass (n_1=1.78) and air interface. A scanning near-field optical microscope (SNOM, NT-MDT) is employed to observe the focal spot near the interface by directly scanning over the focal field. The obstruction arrangement, SNOM head, confocal detecting system, which is not shown in the diagram, and the aluminium coated fiber probe for SNOM have been reported in our previous experiment [12].
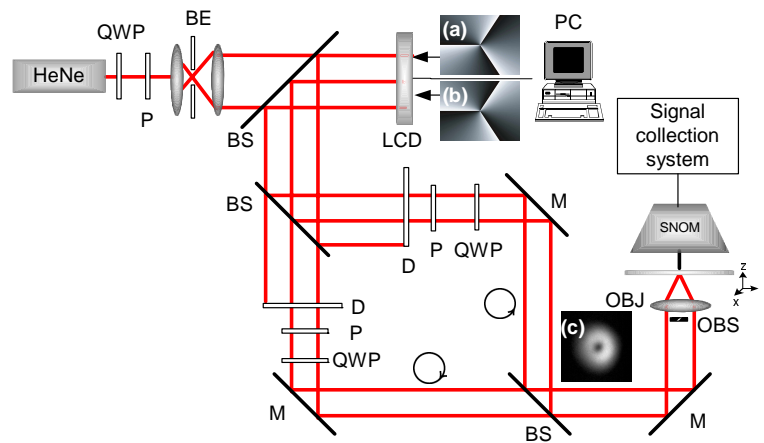
Fig. 1. A schematic diagram of the experimental setup for mapping a tightly focused field of a high NA TIR objective illuminated by a radially polarized beam generated by combining two opposite hand circularly polarized LG beams with opposite topological charges interferometrically under an annular illumination using a SNOM. QWP: quarter wave plate, P: polarizer, BE: beam expansion system, D: diaphragm, BS: beam splitter, M: mirror, OBJ: objective, NA=1.65, 100×, OBS: obstruction. (a), (b) Phase patterns loaded to LCD to produce LG beams with opposite topological charges. (c) The generated radially polarized beam.

3. Results and discussion

To account for the field distribution in the focal region of a high NA objective illuminated by a radially polarized beam through an index mismatched dielectric interface, the vectorial-Debye theory is employed [19,20]. In Fig. 2 the focal field (without any obstruction at the back aperture of the objective) is mapped and compared with the theoretical simulations. It is evident in Fig. 2 inset (a) that for a linearly polarized beam the focal spot elongates along the incident polarization direction due to the depolarization effect in the focal region of a high NA objective [6,12]. However, by using a radial polarization, as shown in Fig. 2(c), such a focus elongation is eliminated, and the intensity distribution in the focal region exhibits a higher lateral resolution due to the strong longitudinal field component of the radially polarized beam, which has a circularly symmetrical distribution. The more accurate analyses have been carried out by comparing the full width at the half maximum (FWHM) of the intensity distribution of the measurements with the theoretical simulations (Fig. 2(e)). It is noted that the FWHM along the polarization direction of a linearly polarized beam is approximately 60

nm broader than the theoretical predication owning to the finite size (60 nm on average) of the detecting probe [12]. This is not unexpected since the mapped focus distribution given by a SNOM probe can be approximated to the convolution of the image with the aperture function of the probe [12]. However, for a radially polarized beam, the experimental result is approximately equal to the calculated total field even without considering the size of the detecting probe. This is due to two factors: first, the weighting of the longitudinal component is significant (over 70% of the total field) in the focal region of an objective lens with NA=1.65 in the case of radially polarized beam illumination. Second, the coupling of the longitudinal polarization component to the aluminium coated fiber probe is approximately three times stronger than that for the transverse polarization component [12]. As a result of the two factors mentioned above, the mapped intensity distribution is dominated by the longitudinal component of the radial field ($|E_z|^2$), which has a narrower distribution (FWHM=185 nm) than that of the total field (FWHM=210 nm) (Fig. 2(e)).
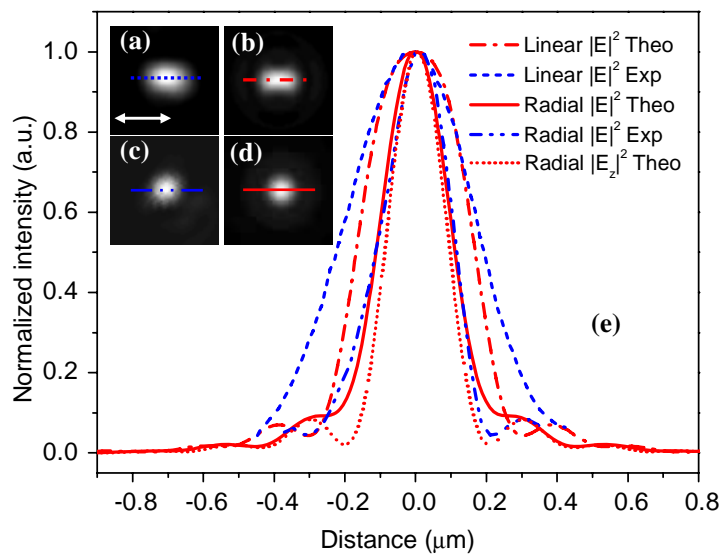
Fig. 2. Comparison of the theoretical predicted and the measured cross-sections of the field intensity distribution in the focal region of the objective under the illumination of a linearly polarized beam and a radially polarized beam. (a) an experimental measurement of a linearly polarized beam, (b) a theoretical prediction of a linearly polarized beam (c) an experimental measurement of a radially polarized beam (d) a theoretical prediction of a radially polarized beam. The arrow indicates the incident polarization direction for a linearly polarized beam. Theo: theory, Exp: experiment.

#8221 - $15.00 USD
(C) 2005 OSA

Received 20 July 2005; revised 19 August 2005; accepted 19 August 2005
5 September 2005 / Vol. 13, No. 18 / OPTICS EXPRESS 6824
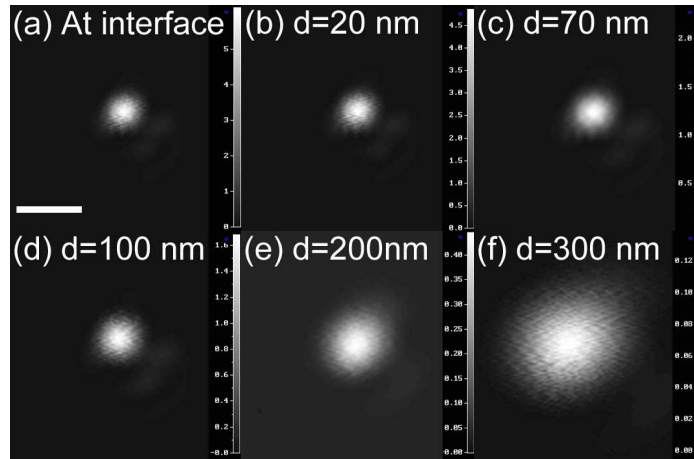
Fig. 3. Measured intensity distributions (normalized by the maximum intensity value) in the focal region of an unobstructed TIR objective illuminated by a radially polarized beam at the horizontal planes of different distances d to the glass-air interface: (a) at interface, (b) $d = 20$ nm, (c) $d = 70$ nm, (d) $d = 100$ nm, (e) $d = 200$ nm, (f) $d = 300$ nm. Scale bar: 500nm.

It should be pointed out that by using the TIR objective, a big portion (more than 65%) of the incident beam satisfies the TIR condition even without inserting any obstruction at the back aperture of the objective. Fig. 3 shows the intensity distributions of the focal field at the interface (Fig. 3(a)) and also shows the intensity distributions of the focal field at planes parallel to the interface with distances d of 20 nm, 70 nm, 100 nm, 200 nm and 300 nm, respectively, away from the interface. It is noticed that the peak intensities of the focus distributions show a pronounced drop from 6 (Fig. 3(a)) to 0.13 (Fig. 3(e)) as the distance increases. When measured at the interface, the focal spot shows a FWHM of approximately 205 nm, which is slightly smaller than the theoretical predication of 210 nm of the total field. As the probe is withdrawn from the surface, the intensity distribution exhibits no change within a certain distance, i.e. 20 nm (Fig. 3(b)), because the evanescent component is still dominant. However, when the distance d is further increased, the evanescent field decays fast and the propagating component becomes dominant. As a result, the field distribution starts to expand and at the same time the intensity drops, as is shown in Fig. 3(c)-(f). When the probe is 200 nm away from the interface, a focal spot with a FWHM of approximately 0.45 μm, which is over twice the size of a near-field focal spot, is observed in the focal region.

The evanescent field is generated in the focal region of the objective using an obstruction disk with a radius $\varepsilon = 0.8$ (normalized by the back aperture of the objective), which is much larger than the critical radius $\varepsilon_c = 0.56$ (corresponding to the critical angle) to ensure that the field is purely evanescent. The measured intensity decay curve shows a perfect match with the theoretical prediction, as is shown in Fig. 4. A decay constant of 48 nm has been obtained both experimentally and theoretically. Several slices of the field intensity distribution have been taken at different distances (d=10 nm, 20 nm, 40 nm, 130 nm) from the interface, as shown in insets (b)-(e) in Fig. 4. The focus splitting phenomenon presented in the case of using linear polarization illumination (Fig. 4(a)) has been removed due to the induction of a radial polarization (Fig. 4(b)). A circularly symmetrical focal spot with a FWHM of 176 nm has been observed at the interface. The lateral size of the focal spot is approximately a quarter of the illumination wavelength, which is only less than half of that under the illumination of a linearly polarized beam. Apart from the intensity decay, the intensity distributions remain unchanged over a certain distance. The focal spots preserve their shapes very well within the near-field region.
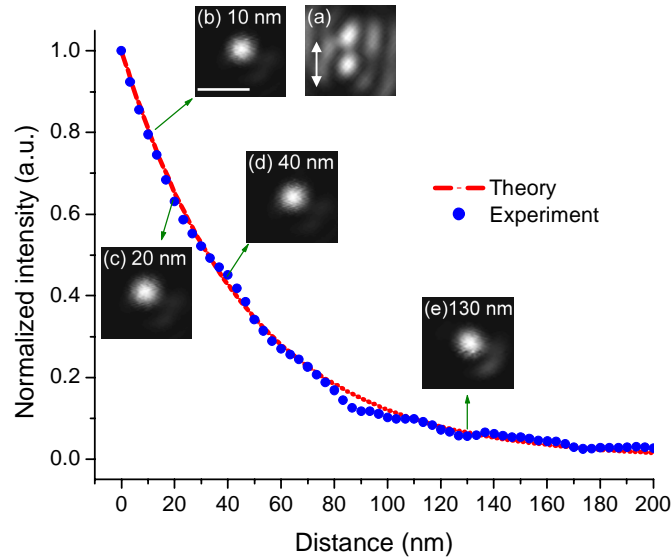
Fig. 4. Experimental and theoretical intensity decay of a purely evanescent focus under the illumination of a radially polarized beam as a function of the tip-sample distance for $\varepsilon=0.8$. Inset (a) focal intensity distribution of a linearly polarized beam, insets (b)-(e) field intensity distributions at the horizontal planes of different distances d to the glass-air interface: (b) $d = 10$ nm, (c) $d = 20$ nm, (d) $d = 40$ nm, (e) $d = 130$ nm. Scale bar: 500 nm. The arrow in inset (a) indicates the incident polarization direction for a linearly polarized beam.

In Fig. 5, the measured FWHM of an unobstructed focus ($\varepsilon = 0$) and an obstructed focus ($\varepsilon = 0.8$) are compared with the theoretically predicted FWHM, and a good match has been demonstrated. As mentioned above, when the probe-interface distance is significant compared to the decay constant of the evanescent field, i.e., d>100 nm, the unobstructed focal spot exhibits an expansion, for example at d=200 nm, the spot size is more than doubled. This originates partially from the defocus effect, which is comparably small (< 10% at d= 200 nm) in this case. The main factor contributing to the broadening is that the propagating component becomes dominant. Taking into account the factors that the weighting of the longitudinal component is less and the effective numerical aperture is small, the propagating field exhibits much broader distribution compared with the near-field component. It is also noted that the FWHM for the obstructed focal spot remains a constant over a distance of 250 nm in Fig. 5. This can be attributed to a combination effect of the strong longitudinal component in the focal region of a radially polarized beam and the non-propagating nature of the evanescent field.
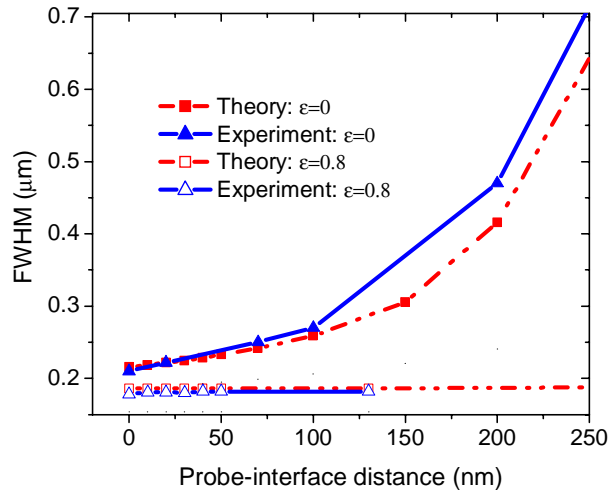
Fig. 5. Comparison of the measured FWHM of the focal spot under unobstructed ($\varepsilon = 0$) and obstructed ($\varepsilon = 0.8$) radial polarization illumination to the theoretical FWHM of the total field.

In summary, the direct measurement of a highly localized evanescent focal spot generated by combining a radially polarized beam with an annular illumination has been demonstrated in this paper. A radially polarized beam is generated by an interferometric method using a single liquid crystal phase modulator, which provides better synchronization in the dynamic control of the focal spot. A focal spot has been confined axially near the interface within a 50 nm range by the fast decaying nature of the evanescent field thus avoiding the focus extending in the axial direction associated with a radially polarized beam illumination. The focus elongation and splitting have been eliminated and the lateral size of the focal spot is approximately a quarter of the illumination wavelength, which is only less than half of that under the illumination of a linearly polarized beam. The technique reported in this paper can find its applications in the field of near-field microscopic imaging and laser trapping, where a high resolution and a high contrast are required simultaneously [7,21].